

Techniques for Measuring the Electromagnetic Shielding Effectiveness of Materials: Part I:—Far-Field Source Simulation

PERRY F. WILSON, MEMBER, IEEE, MARK T. MA, FELLOW, IEEE, AND J. W. ADAMS, SENIOR MEMBER, IEEE

Abstract—Shielding effectiveness relates to the ability of a material to reduce the transmission of propagating fields in order to electromagnetically isolate one region from another. Because the shielding capability of a complex material is difficult to predict, it often must be measured. A number of approaches to simulating a far-field source are studied, including the use of coaxial transmission-line holders and a time-domain system. In each case we consider the system frequency range, test sample requirements, test field type, dynamic range, measurement time required, and analytical background; and present data taken on a common set of materials.

Key Words—coaxial transmission line holder, far-field source simulation, plane wave, shielding effectiveness, shielding materials, time-domain system.

Index Code—F11 d/e/f.

I. INTRODUCTION

THE EFFECTIVE shielding of electronics is a concern of both equipment users and manufacturers. Shielding encompasses a number of different aspects including radiated electromagnetic interference (EMI), conducted EMI, grounding, electrostatic discharge, and environmental effects, all of which contribute to the overall integrity of a system. Shielding here refers to the ability of a material to reduce the transmission of propagating electromagnetic (EM) fields. Shields are used to isolate a region, either to prevent interference from outside sources (susceptibility), or to avoid the leakage of unwanted radiation due to internal sources (emissions). Traditionally, shielding is based on the use of metals with well understood EM properties. However, metals are being increasingly replaced by a variety of less predictable materials. As a result there is significant interest in the development of reliable methods for measuring the shielding effectiveness (SE) of a material. An example serves to illustrate the problem.

Molded plastics have largely replaced metal boxes as the housings for commercial electronic equipment. Plastics alone are inherently transparent to EM radiation; therefore, some metal-like property must be added to insure adequate shielding. Existing approaches include conductive sprays, metal fibers injected during the molding stage, zinc-arc spraying, electro- and electroless-plating, foil inserts, and other metalli-

zation processes [1], [2]. Shielding-associated expenses may well exceed 10 percent of an item's production cost [3]. It is important to make effective choices as to which shielding method is best suited to a particular application, especially where large production runs are planned. Recent FCC regulations applicable to commercial electronics combined with the adverse consequences of failing to pass FCC testing make the need for useful SE data at the design level all the more acute. Similar problems exist in avionics where composites are replacing metal airframes.

Shielding problems involve a variety of EM environments. Therefore, SE measurements seek to either reproduce potential EM conditions, or to yield sufficient information to predict the shield response based on some theoretical model. The basic variables of interest are: 1) frequency, 2) the incident field distribution, and 3) variations in the material under test. A few words about each of these parameters are in order.

Interference sources due to both man-made and natural sources cover a broad spectrum. Much of the present interest is in SE data covering 100 kHz to 1 GHz. This range includes domestic FCC rules governing emissions from computing devices (Code of Federal Regulations, Title 47, Part 15, Subpart J, adopted Oct. 1979), the German VDE 0871/6.78 standard, which is essentially that also proposed by CISPR [4] affecting commercial equipment sold to EEC communities and Japan, and most military requirements such as MIL-STD-461.

Interfering EM fields depend on the source type and location. Susceptibility requirements usually involve EMI originating from distant sources such as communications links, radio transmitters, lightning, etc. Thus, the incident fields are plane wave in nature leading to a need for far-field SE data. On the other hand, emissions problems often involve internal sources close to the shield material. Such near-field sources may be further classified into those that produce a high-impedance field (electric field dominant) such as a short dipole, and those that produce a low-impedance field (magnetic field dominant) like a small loop antenna. The transition point between the near field and the far field, for a simple dipole source, is a distance of approximately $\lambda/2\pi$. Thus, a source which at one frequency is in the near field may become a far-field source at higher frequencies. Actual shielding problems are likely to involve a combination of all of the above conditions. Shielding effectiveness measurement techniques for far-field sources will be the focus of this paper (Part I) while the near-field source simulation problem will be discussed in the companion paper (Part II).

Manuscript received September 1, 1987; revised February 22, 1988.

P. F. Wilson was with the Electromagnetic Fields Division, National Bureau of Standards, Boulder, CO 80303. He is now with ASEA Brown Boveri, Baden/Schweiz, Switzerland.

M. T. Ma and J. W. Adams are with the Electromagnetic Fields Division, National Bureau of Standards, Boulder, CO 80303.

IEEE Log Number 8821923.

Because numerous shielding materials are available, SE test methods need to be flexible enough to allow for different sample types. Materials will vary in thickness, mechanical properties, and cost, as well as electrical properties. Certain test methods require that the sample be of a specific shape to within certain tolerances. This may present a problem if the material is difficult to machine or lacks rigidity. Poor surface conductivity may be a problem if good contact to metal surfaces is necessary for a valid measurement, particularly since most composites and plastic metallizations contain significant amounts of insulating material.

In addition to the variables frequency, incident field type, and test material, other important considerations are the cost of a test system, the time required to obtain data (another form of cost that makes automated test systems desirable), repeatability, and dynamic range. Finally, careful consideration must be given to the interpretation of SE data. Both the intrinsic shielding capabilities of the material as well as the measurement system itself contribute to the resulting SE data [5, Section II]. Explaining this interplay is greatly aided by developing meaningful analytical models of measurement systems whenever possible.

The purpose of any SE test procedure is to quantitatively measure the insertion loss that results from introducing the test sample. The basic arrangement is depicted in Fig. 1. Power from a transmitter (P_T) is coupled to a receiver, first with no material present (P_R) in order to establish a reference level, and then with the sample introduced (P'_R). We will designate measurements performed with the sample in place with a prime. In each case the source output level P_T is kept the same. The ratio of the two received powers gives the insertion loss (IL), typically expressed in decibels

$$IL = 10 \log |P_R/P'_R| \text{ dB.} \quad (1)$$

Beyond this basic definition the particulars of the various SE test procedures vary significantly.

In examining the specific SE measurement methods, we begin in each section with some background on the test configuration, such as the equipment used, dimensions, applicable frequency range, incident test field type, sample requirements, dynamic range, etc. This is followed by an analysis of the system. Whenever applicable a time convention of $\exp(j\omega t)$ is assumed. The shield-material parameters of interest are the thickness d , the conductivity σ , the permeability $\mu = \mu_r \mu_0$, where ϵ_0 and μ_0 are the free-space values and ϵ_r and μ_r are the relative values. In each case we attempt to use the same set of test materials thereby giving us some basis for comparing different methods. Samples include a pair of simple materials, namely, a layer of gold or aluminum on Mylar. Since these materials have well defined electrical properties, they can be used to examine the validity of theoretical models. Known materials also allow us to try and identify those parasitic factors of the measurement system that have not, or cannot be well controlled. In addition, two more complex samples will be tested: a layered plastic-aluminum-plastic fabric-like material, and a graphite-loaded composite. Both these samples feature significant metal content but also have highly insulating surfaces. This allows

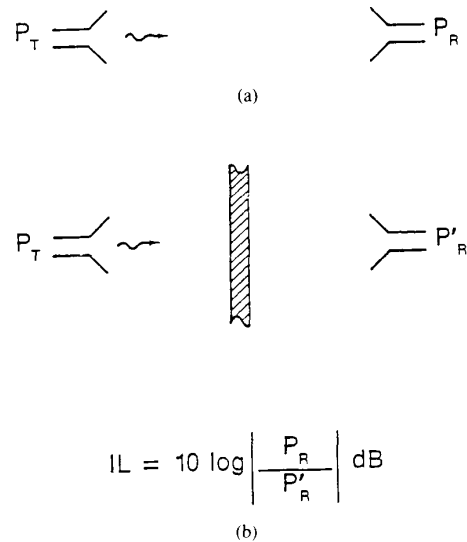


Fig. 1. A typical arrangement for measuring the shielding effectiveness of a material. (a) Unloaded coupling. (b) Loaded coupling.

us to consider the effect of contact impedance and nonhomogeneity.

We will consider two methods based on the use of circular coaxial transmission-line holders. Section II examines a continuous conductor version. The holder is essentially an expanded section of $50-\Omega$ circular coaxial line, operated in the dominant TEM mode. It may be disassembled to allow the insertion of an annular (washer-shaped) test sample. The equations describing reflection and transmission in the coaxial line are equivalent to those describing a free-space plane wave normally incident on an infinite sheet of the sample. Thus, the coaxial holder simulates far-field shielding behavior. The advantage of this approach is both its ease of use and analysis. The primary difficulty is that contact impedance between the sample and the coaxial-holder conductors can significantly degrade the measured results.

Section III considers a second type of circular coaxial holder, a flanged version developed at National Bureau of Standards (NBS). A solid disk of the material is mounted between two large flanges and capacitive coupling is used to propagate the TEM mode through the sample. The unloaded reference measurement involves two pieces of the same material matching the dimensions of the flanges but leaving the space between the inner and outer conductors empty. This tends to overcome the contact impedance problem except at frequencies too low to generate sufficient displacement current. In general, this fixture works well and gives repeatable far-field equivalent IL data. The flanged coaxial holder is a more difficult fixture to model. An equivalent circuit description is considered that enables us to examine factors such as the effect of insulating surfaces.

The two circular coaxial-holder techniques involve the use of waveguides operating in the fundamental TEM mode. Thus, there is an upper frequency limit to their use due to the appearance of higher-order modes. These modes destroy the desired incident field distribution and make the interpretation

of results difficult. In order to gain plane-wave SE data at frequencies above those covered by the coaxial holders, a time-domain technique is considered, as discussed in Section IV. The sample is either a large sheet or small sample mounted over an aperture in a large copper screen. A short pulse is used as the source signal. All unwanted signals to the receiving antenna from reflections and scatterings can be windowed out due to time delays and only the direct-path signal is retained. This procedure makes the sample or the copper sheet appear to be infinite in extent. Time-domain measurements give information at frequencies well above those of the other techniques considered here.

The above methods are those with which the authors have had some direct experience. In Section V we consider some alternative approaches, namely, direct measurements of complex permittivities, rectangular waveguides, and the use of nested reverberating chambers. This list is not meant to be exhaustive.

In the concluding remarks of Section VI we summarize the various SE test system characteristics and their range of applicability. Given the wide variety of potential test conditions and materials it is unlikely that any single method will prove adequate to meet all the measurement demands. Rather, some combination of different approaches will be required. It may well be that the intended use of the sample will dictate which measurement method is "best." Therefore, it is important to examine as many different test approaches as is practical.

II. CIRCULAR COAXIAL TRANSMISSION-LINE HOLDER WITH CONTINUOUS CONDUCTOR

A. Test Configuration

One of the important questions concerning a shield material is how well it shields an incident plane wave. Plane waves result from any source that is located in the far field. A basic requirement in SE testing is to isolate the source and receiving antennas. Since true far-field testing using an infinite sheet of the sample is impractical, alternative methods are necessary. One practical approach is to use a waveguide to excite and receive the fields. This results in a simple, well isolated system. If the waveguide is to simulate a free-space plane wave, then one that supports a TEM mode is the logical choice. This in turn suggests the use of a two-conductor transmission line. These considerations have led to the development of coaxial transmission-line holders for simulating far-field SE testing.

A commonly used coaxial holder is a continuous-conductor (CC) version [6], [7]. As shown in Fig. 2, it consists of a section of expanded $50-\Omega$ line which tapers at each end to mate with ordinary $50-\Omega$ coaxial line. The central section has inner and outer dimensions of 4.35 and 9.90 cm, respectively. The holder may be disassembled to allow the insertion of an annular (washer shaped) testing sample. When assembled, both the inner and outer conductors ideally form continuous connections. The dominant TEM mode has no low-frequency cutoff; the low-frequency limit is determined by equipment. The high-frequency limit is approximately 1.4 GHz and is due to the appearance of resonances associated

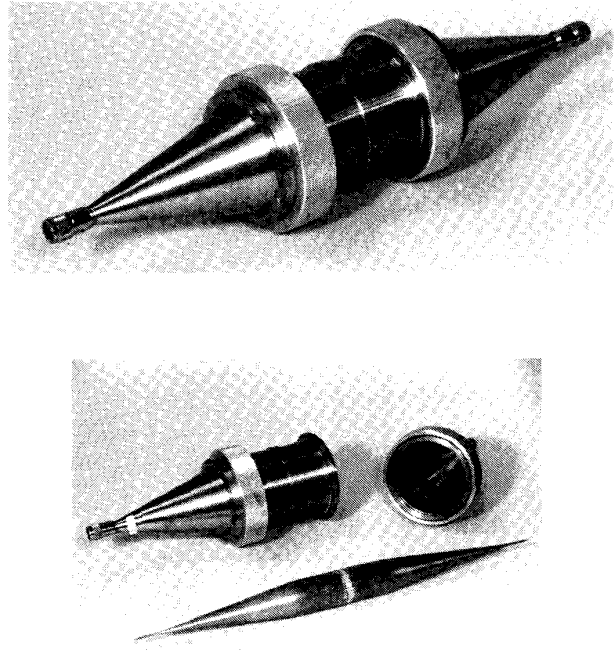


Fig. 2. Continuous-conductor coaxial transmission-line holder.

with the higher-order modes. The dynamic range of this fixture is on the order of 90–100 dB. The CC holder is quite easy to use and lends itself well to an automated system, such as the present NBS bench shown in Fig. 3. The computer controlled system uses a spectrum analyzer to measure incident, reflected, and through powers at frequencies from 1 MHz to 1 GHz (the upper frequency limit of the signal source used). A typical data set (40 frequencies) takes about 15 min to obtain.

B. Analytical Background

A coaxial line such as the CC holder may be analyzed as a length of transmission line with the sample representing a loaded section [5, Appendix A], as shown in Fig. 4. Insertion loss should behave according to

$$IL = 10 \log \left| 1 + \frac{P_{\text{refl}}}{P_t} + \frac{P_{\text{abs}}}{P_t} \right| \quad (2)$$

where P_{refl} and P_{abs} represent the total reflected and absorbed powers (including contributions from internal re-reflections), and P_t is the through power delivered to the end termination in the loaded case. In general, (2) is quite complicated. However, for a thin, conductive sample (2) reduces to [5]

$$IL = 20 \log \left| 1 + \frac{1}{2} \eta_0 \sigma d \right| \quad (3)$$

where η_0 is the free-space wave impedance ($120\pi \Omega$), and σ and d are the material conductivity and thickness. Equation (3) is frequency independent and simply gives the insertion loss due to reflection alone, or alternately put, the impedance mismatch in the line.

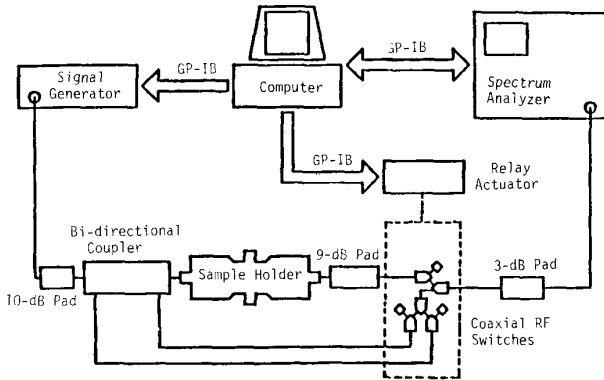


Fig. 3. Block diagram of an automated IL measurement system using a coaxial holder.

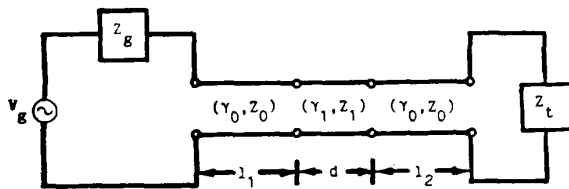


Fig. 4. The continuous-conductor coaxial holder modeled as a reflective transmission line.

A general analysis such as this is typically not used to describe coaxial holders. Rather, most recognize that the coaxial-line approach is primarily a low-frequency device and it is adequate to model the line by a simple circuit as shown in Fig. 5. We then find that the insertion loss should behave according to [7]

$$IL = 20 \log \left| 1 + \frac{Z_0}{2Z_L} \right| \quad (4)$$

where Z_0 is the characteristic impedance of the line (50 Ω) and Z_L is the impedance presented by the load. In the ideal case (a perfect conductor) the sample would present a short across the line and $Z_L \rightarrow 0$ causing an infinite insertion-loss value. If we recognize that the impedance ratio Z_0/Z_L for an electrically thin load should duplicate that of an infinite sheet in free space, then (3) implies that $Z_L = 1/\sigma d$ while $Z_0 = \eta_0$ (intrinsic free-space impedance) and (4) reduces to (3). If we no longer require that the slab be thin, then [8]

$$Z_L Z_0 = -j\eta/(\eta_0 \sin kd) \quad (5)$$

where $\eta = (\mu/\epsilon)^{1/2}$ and $k = \omega(\mu\epsilon)^{1/2}$ are the sample intrinsic impedance and propagation constant.

So far we have assumed that there is no problem insuring good contact between the sample and the coaxial-line conductors. Realistically though, a significant contact impedance may be present. For the CC holder represented by the circuit model shown in Fig. 5, any contact impedance Z_C would appear in series with the load impedance of the sample. That is

$$Z_L \rightarrow Z_L + Z_C \quad (6)$$

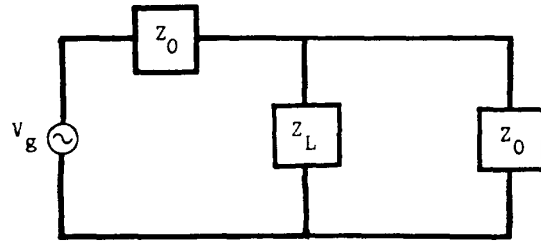


Fig. 5. Idealized coaxial holder transmission-line circuit model.

Under these conditions (4) becomes

$$IL = 20 \log \left| 1 + \frac{Z_0}{2(Z_L + Z_C)} \right| \quad (7)$$

This expression indicates that contact impedance degrades insertion-loss measurements by effectively increasing the impedance of the shield. If the sample is a good conductor (Z_L is small), as in most shield tests, then the effect of Z_C can be significant.

C. Data and Discussion

Figs. 6-9 show the IL data for our basic sample set as measured in the CC holder. Corresponding data from the flanged coaxial holder to be discussed in the next section are also included for comparison purposes. The gold-Mylar data (Fig. 6) show four IL curves; two separate measurements with the annular sample inserted directly into the holder, and two curves involving the silver painting of the sample, either before or after insertion. Apparently, simply placing this sample in the CC holder yields little insertion loss. This may be directly attributed to contact resistance between the sample and the conductors. The gold layer has a quoted σd value of 0.1 S [7]. Thus, based on (3), if we ignore the Mylar, which is radiation transparent, the gold-Mylar sample (which is electrically thin) should yield approximately a flat IL level of 26 dB over this frequency range. Direct insertion results in data well below this expected level and the curve is not well behaved. Users of this particular fixture have recognized that contact resistance degrades measurement data and recommend the use of silver paint to improve contact. However, silver paint can vary in conductivity depending on type and age and one must deal with how much to use and when. The two silver paint curves, before and after insertion, show marked differences. It certainly appears that painting the sample in place gives the highest IL level, but this may be due to excess silver paint deposited on the sample when trying to paint in the confined area of the fixture. In neither case does painting result in a flat curve, suggesting that the presence of the paint introduces a major discontinuity into the line. As silver paint per se is not under test, this is an undesirable effect.

Consider next the aluminum-Mylar sample data shown in Fig. 7. The conductivity and thickness of the aluminum layer are comparable to the above gold-Mylar material and we expect IL data on the order of 20-30 dB. Again silver painting improves results, but both curves fall short of the predicted range. Neither curve is flat as would be expected for an

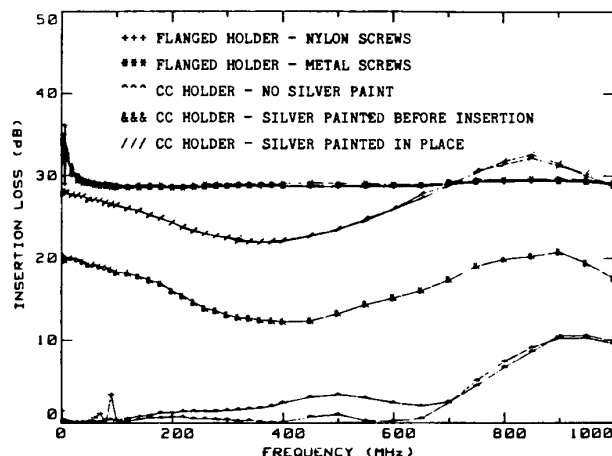


Fig. 6. Insertion loss for the gold-Mylar sample measured in the continuous conductor (CC) and the flanged coaxial holders.

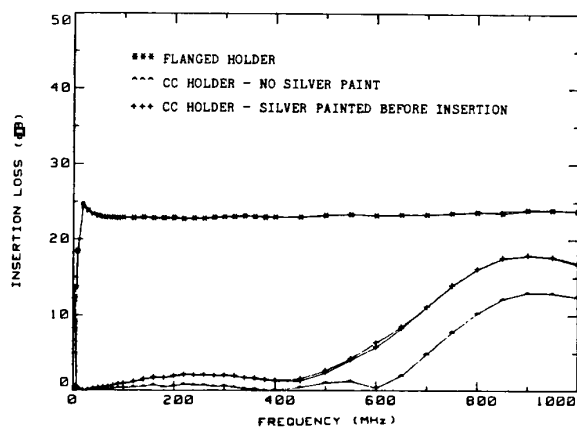


Fig. 7. Insertion loss for the aluminum-Mylar sample measured in the continuous conductor (CC) and the flanged coaxial holders.

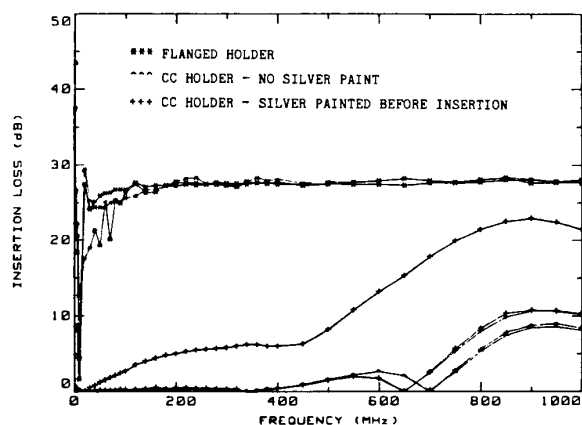


Fig. 8. Insertion loss for the plastic-aluminum-plastic sample measured in the continuous (CC) and the flanged coaxial holders.

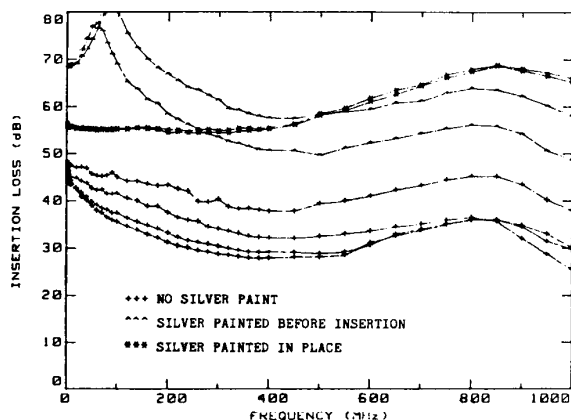


Fig. 9. Insertion loss for the graphite composite sample measured in the continuous conductor (CC) coaxial holder.

electrically thin sample. Fig. 8 shows the plastic-aluminum-plastic data. Here we no longer have a conductive surface on either side. As expected, the direct insertion data are poor despite the aluminum layer between the plastics. Based on the aluminum layer alone, we again expect 20–30 dB of IL. The unpainted IL measurements are for the most part less than 10 dB, well away from the expected range. Silver painting before insertion does help since some contact between the exposed aluminum layer and the test fixture conductors is established, but data are still significantly degraded.

Fluctuations are even worse for the graphite composite sample, shown in Fig. 9 (flanged holder data appear in Fig. 12), although the relative IL level measured is higher. Silver painting improves IL but results are not repeatable. For example, the four unpainted IL data curves differ by up to 10 dB, while painting before insertion still results in variations of approximately 8 dB.

The conclusion one draws from these data is that contact resistance is a major influence when using the CC holder. Silver painting improves IL but the results tend to be short of expected behavior, unpredictable, and often difficult to repeat. The use of silver paint also slows measurement time since the fixture must be carefully cleaned after each use to rid it of unwanted residues. Nonetheless, the coaxial-holder approach remains attractive because of its simplicity and ability to model a far-field SE test. The flanged coaxial holder considered in the next section is an attempt to retain these advantages while better controlling the effects of poor, or variable contact.

III. FLANGED CIRCULAR COAXIAL TRANSMISSION-LINE HOLDER

A. Test Configuration

An alternative to the CC holder is to use flanges to both secure the sample and capacitively couple the conductors, as shown in Fig. 10. The inner conductor of the NBS fixture of this type is 3.2 cm in diameter, while the outer flange has inner and outer diameter dimensions of 7.6 and 13.3 cm, respectively. The sample shape is no longer annular. Instead, two pieces of material are needed. Measurements for the loaded case require a disk shaped sample with a radius equal to that of the outer flange dimension, (13.3 cm). The unloaded reference

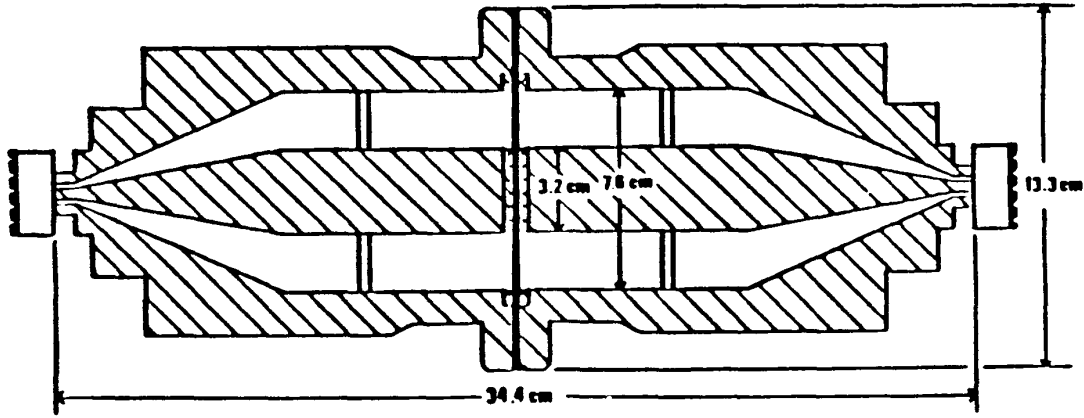


Fig. 10. Flanged coaxial transmission-line holder.

measurement is done with an annular shaped piece of material matching the outer flange dimensions ($7.6 \text{ cm} < \text{diameter} < 13.3 \text{ cm}$), and a disk matching the diameter of the inner conductor. This allows us to repeat the capacitive coupling of the loaded case when establishing the reference level, while leaving the space between the two conductors free (unloaded). Clearly, a significant perturbation is introduced into the line and the analysis of the flanged line is complicated. Nylon screws are used to fasten the flanges together. Metal screws tend to put the contact impedance in series with the test sample as in the CC version. Using nylon screws places at least some of the contact impedance perturbation in parallel with the sample [9]. The frequency range is similar to that of the CC holder, 1 MHz to 1.8 GHz, with the lower end limited by equipment and the upper end determined by the appearance of resonances. The dynamic range is also similar, 90–100 dB. The automated system used to drive the flanged fixture is also the same and the block diagram of Fig. 3 again applies.

B. Analytical Background

The circuit diagram used to model the flanged coaxial holder is shown in Fig. 11. Contact resistance between the flanges and test material are modeled by R_A , R_B , R_E , and R_F . In addition we now have capacitive coupling between the flanges themselves (Z_A , Z_B , Z_E , Z_F) as well as capacitive coupling between the flanges and the sample (Z_C , Z_D). An application of Kirchhoff's voltage law yields the following set of equations for the unknown currents I_1 through I_6 :

$$I_1(Z_0 + R_A + Z_L + R_E) - I_2 Z_L - I_3 R_A - I_5 R_E = V_g$$

$$I_2(Z_0 + R_B + Z_L + R_F) - I_1 Z_L - I_4 R_B - I_6 R_F = 0$$

$$I_3(Z_A + Z_C + R_A) - I_1 R_A - I_4 Z_C = 0$$

$$I_4(Z_B + Z_C + R_B) - I_2 R_B - I_3 Z_C = 0$$

$$I_5(Z_D + Z_E + R_E) - I_1 R_E - I_6 Z_D = 0$$

and

$$I_6(Z_D + Z_F + R_F) - I_2 R_F - I_5 Z_D = 0. \quad (8)$$

These equations need to be solved for I_2 in order to find the

current delivered to the output impedance Z_0 . The result is

$$I_2 = V_g B / (AC - B^2) \quad (9)$$

where

$$A = Z_0 + Z_L + R_B + R_F - \frac{R_B^2(Z_A + Z_C + R_A)}{M} - \frac{R_F^2(Z_E + Z_D + R_E)}{N}$$

$$B = Z_L + \frac{R_A R_B Z_C}{M} + \frac{R_E R_F Z_D}{N},$$

$$C = Z_0 + Z_L + R_A + R_E - \frac{R_A^2(Z_B + Z_C + R_B)}{M} - \frac{R_E^2(Z_F + Z_D + R_F)}{N}$$

$$M = (Z_A + Z_C + R_A)(Z_B + Z_C + R_B) - Z_C^2 \quad (10)$$

and

$$N = (Z_E + Z_D + R_E)(Z_F + Z_D + R_F) - Z_D^2.$$

If we let $A' = A - B$ and $C' = C - B$, that is

$$A' = Z_0 + \frac{R_B[Z_A(Z_B + Z_C) + Z_B(R_A + Z_C)]}{M} + \frac{R_F[Z_E(Z_F + Z_D) + Z_F(R_E + Z_D)]}{N}$$

and

$$C' = Z_0 + \frac{R_A[Z_B(Z_A + Z_C) + Z_A(R_B + Z_C)]}{M} + \frac{R_E[Z_F(Z_E + Z_D) + Z_E(R_F + Z_D)]}{N} \quad (11)$$

then the output current (9) becomes

$$I_2 = V_g \frac{B}{B(A' + C') + A'C'} \quad (12)$$

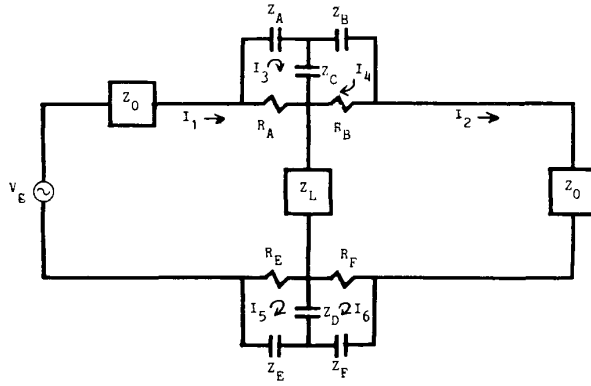


Fig. 11. Flanged coaxial holder circuit model.

The power received at the output (loaded case) is

$$P'_R = \frac{Z_0}{2} |V_g|^2 \left| \frac{B}{B(A' + C') + A'C'} \right|^2. \quad (13)$$

If no sample is present $Z_L \rightarrow \infty$ (open circuit) and consequently $B \rightarrow \infty$. Thus, the unloaded output power is

$$P_R = \frac{Z_0}{2} |V_g|^2 \left| \frac{1}{A' + C'} \right|^2 \quad (14)$$

with the compensation material in place. Combining (13) and (14) implies that insertion loss (1) should behave according to

$$IL = 20 \log \left| 1 + \frac{A'C'}{B(A' + C')} \right|. \quad (15)$$

Let us now examine some special cases. If in fact the system behaves in an ideal sense (perfect contact between the holder and sample), then all the stray impedances (R_A , Z_A , etc.) will be shorted. In this case: $A' \rightarrow Z_0$, $B \rightarrow Z_L$, and $C' \rightarrow Z_0$ and (15) reduces to (4) as expected.

Realistically, these stray impedances will contribute. As the operating frequency increases, the capacitive impedances Z_A , Z_B , Z_E , and Z_F decrease. If $\omega C \gg 1$ these capacitors act much like shorts. Dropping these terms we have

$$\begin{aligned} A' &= C' = Z_0 \\ B &= Z_L + \frac{R_A R_B Z_C}{M'} + \frac{R_E R_F Z_D}{N'} \\ M &= R_A R_B + Z_C(R_A + R_B) \end{aligned} \quad (16)$$

and

$$N = R_E R_F + Z_D(R_E + R_F).$$

The remaining terms depend on the contact resistances between the material and the flanges (R_A , R_B , R_E , R_F) and the capacitive coupling to the material itself (Z_C , Z_D). For a good conducting material Z_L should be small. Thus we may well have the unwanted terms in B of the same order as Z_L . If the material has very good surface conductivity, such that R_A through R_F are zero, then insertion loss tends toward the ideal value (4). In fact we need only have good surface conductivity

on one side, such as R_A , $R_E \approx 0$ or R_B , $R_F \approx 0$ and (16) again yields the ideal insertion loss value (4).

If the material has very poor surface conductivity, such that R_A , $R_B \gg |Z_C|$ and R_E , $R_F \gg |Z_D|$, then B in (16) reduces to

$$B \approx Z_L + Z_C + Z_D \quad (17)$$

and IL becomes

$$IL = 20 \log \left| 1 + \frac{Z_0}{2(Z_L + Z_C + Z_D)} \right|. \quad (18)$$

For shield materials of good conductivity such that $|Z_L| \ll |Z_C|$, $|Z_D|$ we see that unwanted impedances Z_C and Z_D can dominate the insertion loss measurement. It is hoped that these capacitances between the material and the holder will be small for good conductors, even if the surface is insulating.

C. Data and Discussion

Insertion-loss data for our basic samples appear in Figs. 6–8, and 12. In three cases (gold-Mylar, aluminum-Mylar, plastic-aluminum-plastic) the data was flat and highly repeatable. The gold-Mylar data agree well with the predicted values of 26 dB. The differences are likely due to inaccuracy in the quoted $\sigma d = 0.1$ S value for this sample. Contact impedance is probably not the problem or we would expect more fluctuations with frequency. The graphite composite data, shown in Fig. 12, are not as well behaved. This sample is thicker than the others; thus, the capacitances are not as large nor is Z_L as frequency independent. Both metal and nylon screws were used to secure the sample between the flanges. The metal screw measurements show significantly less IL and larger variations. This tends to confirm the use of nylon screws to avoid putting contact resistance in series with the sample. None of the data based on the flanged coaxial holder require the use of silver paint.

A comparison between data from the top coaxial holders indicates that the flanged holder behaves more like the theoretical model described by (3) and (4). The IL data from the flanged holder are less degraded and more repeatable. In addition, for electrically thin samples (3) can be used to empirically estimate σd . For example, Figs. 6–8 show that we measure IL levels of approximately 29, 24, and 28 dB for the gold-Mylar, aluminum-Mylar, and plastic-aluminum-plastic samples, respectively. Inverting (3) yields σd values of 0.144, 0.079, and 0.128 S. In fact, it should be possible to invert the more general expression based on (4) and (5) using a complex root finder if the thickness is known and the relative dielectric constant may be ignored. These can in turn be used to predict the expected IL for other geometries or measurement systems.

IV. TIME-DOMAIN APPROACH

A. Test Configuration

Pulsed (time-domain) sources allow us to differentiate between direct and indirect (diffracted) paths. Efficient FFT algorithms then convert time-domain data to the frequency domain for comparison to data obtained using CW sources. We will define clean time as the interval between the arrival of the desired direct-path signal and the first unwanted indirect-

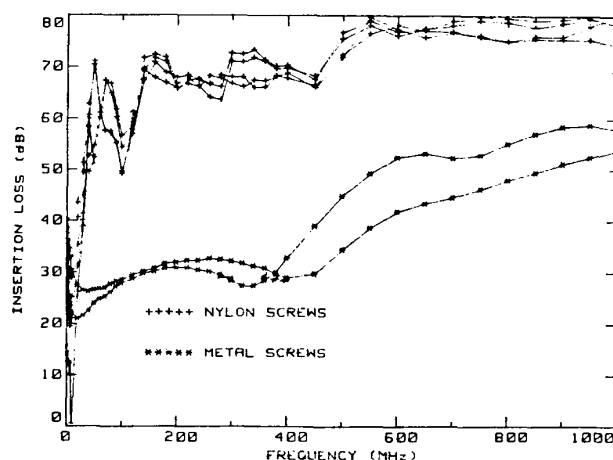


Fig. 12. Insertion loss for the graphite composite sample measured in the flanged coaxial holder.

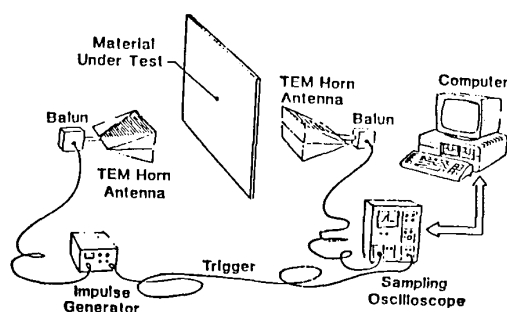


Fig. 13. The time-domain shielding effectiveness measurement system.

path signal. Longer clean time results in data covering a wider frequency range. The present NBS system, shown in Fig. 13, uses TEM horn antennas spaced 30 cm from the test material with a 350-ps pulse as the input. The direct path fields will be approximately plane wave if the antennas are in the far-field region of the sample (in this case for frequencies above 160 MHz). If the antennas are in the near-field range of the test sample, it will be difficult to predict the incident field type as well as any impedance loading effect the sample may have on the source antenna itself. The high-frequency limit to the present system, 3.5 GHz, is significantly higher than the other methods considered here. The low-frequency limit is determined by the clean time and the far-field condition and at present is approximately 200 MHz. The use of shorter pulses would allow the high-frequency end to be extended. The dynamic range is only 50–60 dB. Thus, this method may not be applicable to extremely good shield materials. The FFT can convert the time-domain signature to the frequency domain very quickly.

Ideally, large sheets should be available for use with this method as shown in Fig. 13. Small samples do not yield sufficient clean time to obtain meaningful data. If small samples are to be tested we must resort to an aperture measurement. NBS has a large copper plane (2.5×2.8 m) with a centrally located circular aperture of diameter 7.6 cm (3 in). A 15.2 cm (6 in) square acrylic plastic plate is used to

press the sample against the aperture and is itself attached to the copper screen using four nylon screws. This configuration yields adequate clean time but introduces the unwanted complication of aperture coupling. At high frequencies the aperture is electrically large and a simple analytical solution is not available.

B. Analytical Background

Pulse penetration through apertures and slabs has received considerable attention due to the interest in electromagnetic pulse (EMP) shielding. A good review of the problem is given by Karzas and Mo [10]. The problem may be formulated in terms of a sequence of transmission functions [11]: propagation from the antenna to the sample (P_1), transmission through the sample (T), through the aperture (A), and to the receiving antenna (P_2). In the time domain these combine to give the overall attenuation of the system by computing a convolution integral. However, in the frequency domain convolution is replaced by multiplication. Formally we may represent the power coupled between the source (P_T) and receiving (P_R) antennas as

$$P_R'/P_T = 20 \log |P_1(k_0 l_1) \cdot T(\sigma, k_0 d) \cdot A(k_0 r) \cdot P_2(k_0 l_2)| \quad (19)$$

where l_1 and l_2 are the distances to the source and receive antennas, and we assume a circular aperture of radius r . If no test material is present, $T(\sigma, k_0 d)$ is replaced with 1. This representation implies that for a large sheet, we have

$$IL = 20 \log \left| \frac{P_1(k_0 l_1) \cdot P_2(k_0 l_2)}{P_1(k_0 l_1) \cdot T(\sigma, k_0 d) \cdot P_2(k_0 l_2)} \right| \\ = -20 \log |T(\sigma, k_0 d)|. \quad (20)$$

For a highly conductive test sample excited by a normal plane wave [11]

$$T(\sigma, k_0, d) = -2j\eta/(\eta_0 \sin kd) \quad (21)$$

where T is normalized to the incident field strength of the no shield case. If $|kd|$ is small (electrically thin sheet) then (20) and (21) combine to give

$$IL \approx 20 \log \left| \frac{1}{2} \eta_0 \sigma d \right| \quad (22)$$

which agrees with the coaxial-holder expression (3) if $\eta_0 \sigma d \gg 1$ (i.e., a good conductor). Thus, for conductive test sheets the time-domain measurements should be similar to those obtained in the coaxial holder.

The addition of an aperture alters the situation only slightly. Referring to (20) we see that the only term affected by loading the aperture is again $T(\sigma, k_0 d)$. The difficulty here is that $T(\sigma, k_0 d)$ may not be readily known. If the sample is located on the source side, then we essentially have plane-wave attenuation preceding the aperture excitation $A(k_0 r)$ and (21) again applies. This ignores the small size of the sample, contact impedances if any, sample resonances, and so on. But as a first approximation we should expect a sample mounted on the

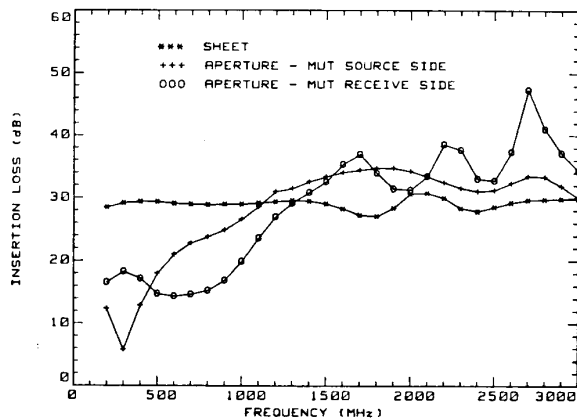


Fig. 14. Insertion loss for the aluminum-Mylar sample (large sheet and 7.6-cm aperture) measured with the time-domain system.

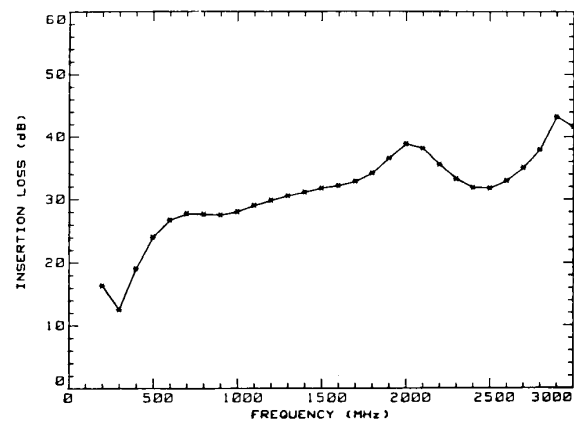


Fig. 16. Insertion loss for the gold-Mylar sample (source side over and aperture) measured with the time-domain system.

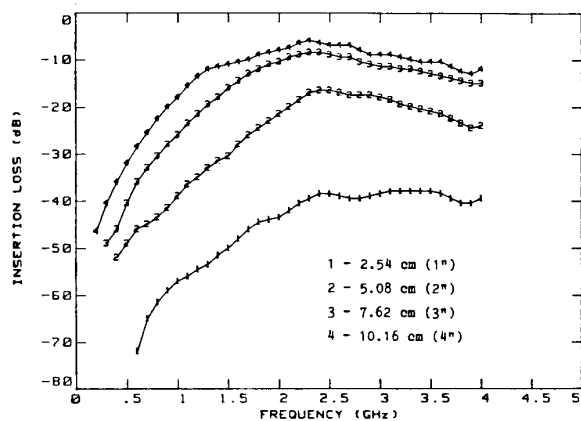


Fig. 15. Tie-domain signal coupling between horn antennas for various empty aperture sizes.

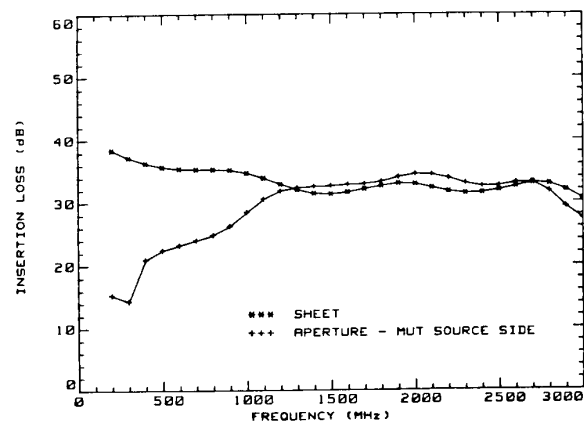


Fig. 17. Insertion loss for the plastic-aluminum-plastic sample (large sheet and source side over an aperture) measured with the time-domain system.

source side of an aperture to yield IL data similar to that for a large sheet. If the sample is mounted on the other side facing the receiving antenna, the aperture fields rather than a plane wave will excite the material. In this case it is difficult to predict $T(\sigma, k_0 d)$. Aperture resonances will also cause the impedance of the exciting field to vary and consequently the IL data being measured. The above considerations suggest that time-domain measurements with aperture on a large copper plane are better performed with the sample mounted on the source side.

C. Data and Discussion

The IL data obtained by the time-domain technique are shown in Figs. 14 and 16–18. The aluminum-Mylar sample in Fig. 14 was measured using all three configurations discussed above, namely, a large sheet (* curve) and aperture loading of sample material both on the source (+ curve) and receiving (O curve) sides. The large sheet curve is basically flat at about 29 dB from 0.2–1.5 GHz whereupon some undulating begins to occur. The IL measured here is somewhat higher than the 24 dB found using the flanged coaxial holder (* curve in Fig. 7). This is probably due to variations in the aluminum layer thickness between the small sample used in the coaxial holder

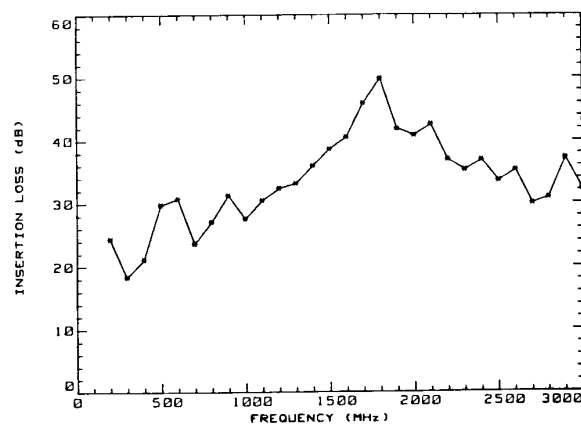


Fig. 18. Insertion loss for the graphite composite sample (source side over an aperture) measured with the time-domain system.

and the large sheet used in the time-domain measurement. In either case agreement within 5 dB is reasonable in the present context. When the sample is placed on the aperture facing the source antenna side, we see some agreement with the large sheet data (< 10 dB) above 1.0 GHz, but with a marked

decrease in the IL measured below 1.0 GHz. The equivalence of these two measurements was predicted above based on the transmission function argument. The agreement is considered reasonable especially when the possible effects of small sample size are recognized. Below 1.0 GHz we may see the loss of dynamic range. This can be demonstrated by examining empty aperture coupling relative to direct coupling (no screen) for various sized apertures, as shown in Fig. 15. Below 1.5 GHz the received signal decreases rapidly, as expected from theory [12], [13]. When the sample is introduced and attenuation is increased, we likely encounter the noise floor at the lower frequencies. When the loaded signal is subtracted from the unloaded signal, we are in fact just subtracting the noise floor and we will show little IL if the unloaded signal is near the noise floor as may be the case here at the lower frequencies. Returning to Fig. 14, we examine a third curve showing IL data for the sample mounted on the receiving antenna side. Again we see the roll off caused by loss of dynamic range below 1.0 GHz and, in addition, the relatively large spikes at 1.7, 2.3, and 2.7 GHz. These may be due to either aperture resonances or to the sample itself resonating like a patch antenna. If we use λ as an estimate of the circumferential resonant length, then aperture resonances would appear at multiples of 1252 MHz (aperture diameter = 7.6 cm) while patch resonances based on a full-wavelength side length of 15.2 cm would appear at multiples of 1968 MHz. The curve here does not clearly agree with either of these values; however, it is reasonable to believe that aperture resonances are the primary cause of the beating behavior observed. Regardless, these curves together indicate that mounting the sample on the source antenna side is likely to yield more meaningful results.

Fig. 16 presents IL data for the gold-Mylar sample mounted on the source side of the aperture. Again we see the low-frequency roll off. The two peaks near 2.0 and 2.9 GHz conform somewhat to the peaks of the aluminum-Mylar sample measured either as a large sheet or over an aperture with the sample on the source side. This indicates that the effect is independent of both the aperture and the sample size. Thus, we are likely observing a nonlinearity in the source signal itself.

Fig. 17 gives IL data of the plastic-aluminum-plastic material both for a large sheet (* curve) and a source side aperture (+ curve) measurements. Here the data agree very well above 1.0 GHz tracking at about 31 dB. This again is a higher IL level than obtained in the coaxial holder (28 dB, * curve in Fig. 8) but not significantly. Measurements on the graphite composite material appear in Fig. 18. The graphite composite data are by no means smooth with distinct spikes at 1.8 and 2.9 GHz. These align somewhat with the signal variations discussed above but are significantly more pronounced. Above 1.0 GHz the graphite composite IL is 30–50 dB. This is lower than the 55–80 dB measured in the flanged holder and the difference is probably due to pushing the dynamic range of the system.

The time-domain approach is fast, broad-band, and compatible with other plane-wave simulation techniques, especially

when a large sheet of the sample is available. Aperture coupling using small samples appears to give reasonable results above 1.0 GHz, but is not as well behaved. Unfortunately, some components of the present system are in the developmental stage. Thus, this method is not well suited for widespread use in the near future.

V. OTHER METHODS

The methods studied in the preceding sections (for simulating far-field source SE) by no means form an exhaustive list. In the context of the present study, some additional techniques are briefly discussed as follows.

A. Complex Permittivity Measurements

If the complex permittivity of a material can be measured directly, then one could predict shielding effectiveness under a variety of conditions [14]–[22]. Far-field SE could be predicted based on (21). Unfortunately, complex permittivity measurements in the microwave frequency range are problematic [23]. Bridge networks are difficult if not impossible to balance in the case of highly lossy materials and their use is usually limited to below 100 MHz. Open and disk resonators extend to much higher frequencies; however, these also tend to be valid only for low-loss materials and not the highly conductive composites often of interest here. Variable length and truncated transmission-line fixtures may be used in the gigahertz range but are more suited to liquids and amorphous materials [24], [25]. These measurements will also yield some type of bulk permittivity that may lead to poor SE predictions for nonisotropic and inhomogeneous materials. Nonetheless, a general method for complex permittivity measurements would be valuable when available.

B. Rectangular Waveguides

It may be possible to perform IL measurements at microwave frequencies by loading rectangular waveguides operating in the TE_{10} mode, much as is done with the coaxial holders. The sample would have to be cut to fit the guide but this should be no more difficult than with most methods. Various sized waveguides could be used to achieve broad frequency coverage. One advantage to this approach is that contact impedance should not be a problem since we are not trying to create a short across a transmission line. Instead, viewing the IL measurement as a microwave circuit problem, we are measuring the scattering-matrix parameters due to introducing the sample. A difficulty is that this method would not simulate any of the standard shield tests: high impedance, low impedance, or plane wave. The TE_{10} mode consists of two magnetic- and one electric-field components. These cannot be separated; thus, we are not considering a near-field IL test. Furthermore, the wave impedance is a function of frequency, as opposed to a plane wave or TEM mode. Thus, these measurements would not readily relate to free-space shielding simulation. If one could interpret results with respect to our needs of standard SE information, this approach might prove to be quite useful. This would likely require using the measurement data to determine

TABLE I
SUMMARY OF THE FAR-FIELD SIMULATION SE TEST METHODS (LBE: LIMITED BY EQUIPMENT)

SE Test Method	Frequency Limit		Field-Type Simulation	Requirements on Samples Under Test	Theoretical Support for Data	Dynamic Range (dB)	Repeatability	Time Required for Measurement
	Low	High						
CC Coaxial Holder	1 MHz (LBE)	1.4 GHz	Normal Plane Wave	Annular Disk	Good	90-100	Moderate or Poor	Min.
Flanged Coaxial Holder	1 MHz (LBE)	1.8 GHz	Normal Plane Wave	Circular + Reference (Ring & Disk)	Good	90-100	Good	Min.
Time-Domain Tech.	200 MHz	3.5 GHz (LBE)	Normal Plane Wave	Large Sheet	Good	50-60	Good	Min.
				Mounted on Aperture	Moderate	40-50	Good	Min.

the complex permittivity of the material and from there its SE, as in Section V-A.

C. Nested Reverberating Chambers

A reverberating chamber is a shielded room (box) with a rotating paddle added [26], [27]. It operates on much the same principle as a microwave oven. Power is injected into the chamber by a transmitting antenna. As the paddle rotates the field structure at any given point changes due to the varying excitation of the cavity modes. However, the average field over numerous paddle positions tends toward a plane-wave behavior. Thus, in a statistical sense the reverberating chamber simulates a free-space environment. Some thought is being given to the use of nested reverberation chambers, one inside the other, to explore material SE [28]. The advantages would be a high dynamic range with low input power since the chambers are high Q cavities, large bandwidth above some low-frequency limit determined by the cell sizes (available modes for mixing), and a relative insensitivity to material inhomogeneities. The disadvantages would be that the reverberating chamber is a specialized facility, and that data acquisition is slow since the concept depends on the averaging of a large number of samples. Nonetheless, this approach holds considerable promise.

VI. CONCLUSION

Approaches for measuring the shielding effectiveness of materials by simulating a far-field source have been studied and experience has been gained as to their relative advantages and disadvantages. The basic characteristics of each method are summarized in Table I. This study has shown that the flanged coaxial holder offers a clear advantage over the continuous-conductor version in measurement repeatability. The upper-frequency limit for both coaxial holders is determined by their dimensions. The time-domain method has been demonstrated as a potential, effective measurement technique in the future, especially for much higher frequencies.

ACKNOWLEDGMENT

The authors would like to recognize both E. J. Vanzura and A. R. Ondrejka of NBS for their careful measurements, which yielded data included in this manuscript.

REFERENCES

- [1] M. B. Miller, "Materials and techniques used in EMI/RFI shielding of plastic chassis for electronic systems," in *SPE Shielding Plastics Symp. Rec.* (Chicago, IL), pp. 139-150, June 1984.
- [2] P. J. Mooney, "Plastics EMI shielding: the evolving state of the art," *EMC Techn.*, vol. 4, pp. 19-28, Oct.-Dec. 1985.
- [3] H. W. Armstrong, "The long term environmental effects upon conductive coatings for plastic enclosures," in *MIDCON Symp. Rec.* (Dallas, TX), pp. 28/2/1-5, Nov. 1982.
- [4] N. May, "RFI shielding of enclosures," *Electron. Eng.*, vol. 55, pp. 77-78, May 1983.
- [5] P. F. Wilson and M. T. Ma, "A study of techniques for measuring the electromagnetic shielding effectiveness of materials," Nat. Bur. Stand., Boulder, CO, NBS Tech. Note 1095, May 1986.
- [6] L. C. Oberholtzer, A. J. Mauriello, and D. E. Stutz, "A treatise on the new ASTM ESI shielding standard," *ITEM*, pp. 174-178, 1984.
- [7] R. M. Simon and D. Stutz, "Test methods for shielding materials," *EMC Techn.*, vol. 2, no. 4, pp. 39-48, Oct.-Dec. 1983.
- [8] J. A. Birkin, R. F. Wallenberg, and O. Milton, "Advanced composite aircraft electromagnetic design and synthesis," in *IEEE Int. Electromagn. Compat. Symp. Rec.* (Boulder, CO), pp. 562-569, Aug. 1981.
- [9] R. A. Week, "Thin-film shielding for microcircuit applications and a useful laboratory tool for plane-wave shielding evaluations," *IEEE Trans. Electromagn. Compat.*, vol. EMC-10, no. 1, pp. 105-112, Mar. 1968.
- [10] W. J. Karzas and T. C. Mo, "Linear and nonlinear diffusion through a ferromagnetic conducting slab," *IEEE Trans. Antennas Propagat.*, vol. AP-26, no. 1, pp. 118-129, Jan. 1978.
- [11] G. Franceschetti and C. H. Papas, "Steady state and transient electromagnetic coupling through slabs," *IEEE Trans. Antennas Propagat.*, vol. AP-27, no. 9, pp. 590-596, Sept. 1979.
- [12] N. Ari, D. Hansen, and H. Schar, "Electromagnetic pulse (EMP) penetration through circular apertures in the frequency domain," *Proc. IEEE*, vol. 73, no. 2, pp. 368-369, Feb. 1985.
- [13] W. T. Cathey, "Approximate expressions for field penetration through circular apertures," *IEEE Trans. Electromagn. Compat.*, vol. EMC-25, no. 3, pp. 339-345, Aug. 1983.
- [14] S. A. Schkunoff, *Electromagnetic Waves*. New York: Van Nostrand, pp. 305-315, 1943.
- [15] R. B. Cowdell, "New dimensions in shielding," *IEEE Trans. Electromagn. Compat.*, vol. EMC-10, no. 1, pp. 158-167, Mar. 1968.
- [16] W. A. Stirrat, "USAECOM contributions to shielding theory," *IEEE Trans. Electromagn. Compat.*, vol. EMC-10, no. 1, pp. 63-66, Mar. 1968.
- [17] R. B. Schulz, V. C. Plantz, and D. R. Brush, "Low-frequency shielding resonance," *IEEE Trans. Electromagn. Compat.*, vol. EMC-10, no. 1, pp. 7-15, Mar. 1968.
- [18] L. F. Babcock, "Computer determination of electromagnetic wave shielding effectiveness," *IEEE Trans. Electromagn. Compat.*, vol. EMC-10, no. 1, pp. 331-334, Mar. 1968.
- [19] S. Levy, "Electromagnetic shielding effect of an infinite plane conducting sheet placed between circular coaxial coils," *Proc. IRE*, vol. 24, pp. 923-941, June 1936.
- [20] J. R. Moser, "Low-frequency shielding of a circular loop electromagnetic field source," *IEEE Trans. Electromagn. Compat.*, vol. EMC-9, no. 1, pp. 6-18, Mar. 1967.

- [21] P. R. Bannister, "New theoretical expressions for predicting shielding effectiveness for the plane shield case," *IEEE Trans. Electromagn. Compat.*, vol. EMC-10, no. 1, pp. 2-7, Mar. 1968.
 - [22] —, "Further notes for predicting shielding effectiveness for the plane shield case," *IEEE Trans. Electromagn. Compat.*, vol. EMC-11, no. 2, pp. 50-53, May 1969.
 - [23] R. H. Clarke and C. B. Rosenberg, "Fabry-Perot and open resonators at microwave and millimeter wave frequencies, 2-300 GHz," *J. Phys. E: Sci. Instrum.*, vol. 15, pp. 9-24, Jan. 1982.
 - [24] H. E. Bussey, "Dielectric measurements in a shielded open circuit coaxial line," *IEEE Trans. Instrum. Meas.*, vol. IM-29, no. 2, pp. 120-124, June 1980.
 - [25] L. Zanforlin, "Permittivity measurements of lossy liquids at millimeter-wave frequencies," *IEEE Trans. Microwave Theory Tech.*, vol. MTT-31, no. 5, pp. 417-419, May 1985.
 - [26] M. L. Crawford and G. H. Koepke, "Design, evaluation, and use of a reverberation chamber for performing electromagnetics susceptibility/vulnerability measurements," Nat. Bur. Stand., Boulder, CO, NBS Tech. Note 1092, Apr. 1986.
 - [27] M. T. Ma, M. Kanda, M. L. Crawford, and E. B. Larson, "A review of electromagnetic compatibility/interference measurement methodologies," *Proc. IEEE*, vol. 73, no. 3, pp. 388-411, Mar. 1985.
 - [28] M. O. Hatfield, "Shielding effectiveness measurements using mode-stirred chambers—A comparison of two approaches," see this issue.
-